analytical chemistry

Open Access
This article is licensed under CC-BY-NC-ND 4.0

pubs.acs.org/ac
Article

MINNO: An Open Source Software for Refining Metabolic Networks and Investigating Complex Network Activity Using Empirical Metabolomics Data

Ayush Mandwal, Stephanie L. Bishop, Mildred Castellanos, Anika Westlund, George Chaconas, Jörn Davidsen,* and Ian A. Lewis*

Cite This: *Anal. Chem.* 2024, 96, 3382−3388
Read Online

ACCESS | Metrics & More | Article Recommendations | Supporting Information

ABSTRACT: Metabolomics is a powerful tool for uncovering biochemical diversity in a wide range of organisms. Metabolic network modeling is commonly used to frame metabolomics data in the context of a broader biological system. However, network modeling of poorly characterized nonmodel organisms remains challenging due to gene homology mismatches which lead to network architecture errors. To address this, we developed the Metabolic Interactive Nodular Network for Omics (MINNO), a web-based mapping tool that uses empirical metabolomics data to refine metabolic networks. MINNO allows users to create, modify, and interact with metabolic pathway visualizations for thousands of organisms, in both individual and multispecies contexts. Herein, we illustrate the use of MINNO in elucidating the metabolic networks of understudied species, such as those of the *Borrelia* genus, which cause Lyme and relapsing fever diseases. Using a hybrid genomics-metabolomics modeling approach, we constructed species-specific metabolic networks for three*Borrelia* species. Using these empirically refined networks, we were able to metabolically differentiate these species via their nucleotide metabolism, which cannot be predicted from genomic networks. Additionally, using MINNO, we identified 18 missing reactions from the KEGG database, of which nine were supported by the primary literature. These examples illustrate the use of metabolomics for the empirical refining of genetically constructed networks and show how MINNO can be used to study nonmodel organisms.

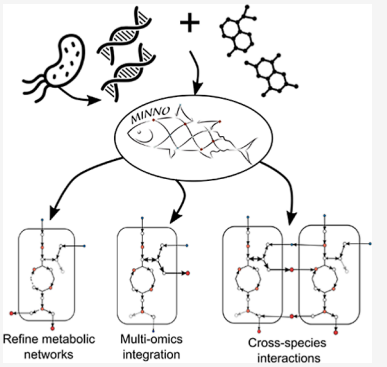

Downloaded via 184.144.125.2 on January 2, 2025 at 18:11:57 (UTC).
See https://pubs.acs.org/sharingguidelines for options on how to legitimately share published articles.

Metabolomics has emerged as a mainstream approach for investigating a diverse range of biological phenomena and exploring the molecular underpinnings of disease.[1,2] One of the core underlying tools used in metabolomics research is metabolic network modeling, which is used to place metabolic data in the context of an organism's overall metabolic network.[3] Although the core elements of metabolism are shared between most living organisms (e.g., central carbon metabolism), species-to-species diversity can contribute to significant differences in nutritional preferences.[4,5] These differences are especially important in the context of evolution, where natural selection has driven organisms to streamline their metabolic networks according to the specific niches they inhabit.[6]

Currently, most metabolic networks are derived from a handful of model organisms such as *Escherichia coli*, *Saccharomyces cerevisiae*, or *Mus musculus*. Species-specific networks are then constructed from genomic homology searches using tools such as the prokaryotic genome annotation pipeline (PGAP),[7,8] which identify the most likely enzyme for each reaction in the network.[9] Although this strategy works well in species that are closely related to these model organisms, it is less effective when applied to species that are highly divergent from the original model.[10] Mismatches due to poor homology result in missing enzymes in the metabolic network, which, without further data refinement, can be misinterpreted as metabolic deficiencies.[11,12] This is a critical problem for understanding the evolution of microbes and for making inferences about the metabolic architecture of nonmodel organisms.

Another major challenge in investigating nonmodel organisms is that existing network visualization tools make it difficult to integrate multiomics data to tune genomic networks. Although several visualization tools have been developed such as Escher,[13] MetExploreViz,[14] Omix,[15] Cytoscape,[16] CellDesigner,[17] and PathVisio,[18] they all suffer from a lack of scalability and reusability. None of these tools come with a generic base network architecture that can be used to build the network of any organism, and they often require bioinformatics or coding skills to alter existing networks.[15,17]

Received: October 6, 2023
Revised: December 18, 2023
Accepted: January 19, 2024
Published: February 15, 2024

ACS Publications
© 2024 The Authors. Published by American Chemical Society

https://doi.org/10.1021/acs.analchem.3c04501
Anal. Chem. 2024, 96, 3382−3388

When expanding metabolic networks by adding more pathways, users are typically required to manually add them one by one or reorganize the network if the initial layout is lacking.[13,14,16,18]

To address these challenges, we developed the JavaScript-based web application Metabolic Interactive Nodular Network for Omics (MINNO). MINNO promotes network reusability by offering base networks that serve as a foundation for overlaying organism-specific networks. Moreover, it enables the integration of diverse metabolic pathways in a modular fashion, eliminating the need for coding or extensive reorganization of the entire combined network. These capabilities enhance the scalability of network construction and facilitate empirical data-driven refinement of metabolic networks. As a proof-of-concept, we used MINNO to conduct an empirical refinement of three metabolic pathways for three species of *Borrelia*, spirochetes that cause Lyme disease and relapsing fever in humans and other vertebrates.[9,20] *Borrelia* spirochetes follow a complex life cycle in which they are sequentially passed from ticks to a mammalian host.[21,22] These species are obligate parasites, and selective pressure has streamlined their metabolic networks to dispense with the biosynthesis of many metabolites that can be obtained directly from their host.[19,20] Using MINNO, we found evidence for metabolic streamlining and divergence among Lyme disease and relapsing fever spirochetes resulting from these specific host/vector interactions.

In summary, the construction of metabolic networks for nonmodel organisms using genomics analysis is hindered by homology mismatches, which present a critical challenge in understanding microbial evolution and inferring their metabolic architecture. Existing visualization tools lack the necessary scalability and reusability features to effectively integrate multiomics data into the network, thereby impeding network refinement. To address these limitations, MINNO utilizes a hybrid genomics-metabolomics strategy that incorporates metabolic boundary flux analysis, genomic network projection, and empirical refinement based on metabolic data and will thus facilitate the study of a significantly broader range of nonmodel species.

MATERIALS AND METHODS

Microbial Growth and Sample Preparation. The *Borrelia* strains used in this study were *Borrelia burgdorferi* B31 5A4 (GCB921),[23] *Borrelia turicatae* 91E135 (GCB801), and *Borrelia parkeri* RML (GCB803).[24] For the extracellular metabolite temporal profiling data set, all strains were propagated in BSK-II medium prepared in-house and supplemented glucose and glycerol or a combination of uniformly labeled ^{13}C glucose (D-glucose U-$^{13}C_6$, Cambridge Isotope Laboratories, Tewksbury, MA, USA) or uniformly labeled ^{13}C glycerol (glycerol $^{13}C_3$, Sigma Aldrich, Oakville, ON, Canada) with 6% rabbit serum.[25] When the cultures approached log phase (1 to 5×10^7), we diluted them in BSK-II with 6% rabbit serum to 1×10^5 spirochetes/mL. We used 96-well plates (Life Science BRAND, Fisher Scientific, Toronto, ON, Canada) to grow triplicate samples of 250 μL for time points 0 and 72 h and incubated them in a Forma Series II Water-Jacketed CO_2 Incubator (Thermo Scientific, Waltham, MA, USA) under conditions of 35 °C and 1.5% CO_2. At each time point, we transferred the cultures to 1.5 mL Eppendorf tubes and centrifuged them for 10 min at 13,000 rpm in a mini-centrifuge 5415 R (Eppendorf, Mississauga, ON, Canada), followed by removal of 100 μL of the supernatant and mixing it with an equal volume of 100% HPLC grade methanol (EMD Millipore, Oakville, ON, Canada). We then centrifuged the samples again under the above conditions and diluted the supernatant 1:10 with 50% LC−MS grade methanol (with 50% LC−MS grade water) to prepare the extracts for liquid chromatography−mass spectrometry (LC−MS) analysis.

Metabolomics Analysis. We performed all metabolomics analyses at the Calgary Metabolomics Research Facility (CMRF), as described in detail in refs 26 and 27. In brief, compounds were separated via hydrophilic interaction liquid chromatography (HILIC) with a 100 mm × 2.1 mm Syncronis HILIC column (2.1 μm particle size; Thermo Fisher Scientific) using a Thermo Fisher Scientific Vanquish UHPLC platform and a Thermo Scientific Q Exactive HF Hybrid Quadrupole-Orbitrap mass spectrometer. To ensure LC−MS system stability, the HILIC column was conditioned with ∼400 replicate injections of a biological control sample before use, and all solvents were produced and pH-adjusted in one batch to minimize solvent batch effects.[27] Raw MS data were converted to mzXML file format using MSConvert GUI software[28] and analyzed using El-Maven (El-MAVEN v0.12.0).[29] Metabolites were identified by comparison to an in-house metabolite library optimized for our instrumental setup (MetaSci, Toronto, ON, Canada) or quantified by comparison to standard solutions prepared from compounds ordered from Sigma-Aldrich, using external standard curves. Compound CAS numbers and standard curve parameters used for concentration calculations are included in the Supporting Information files.

For quantitative estimation of metabolic boundary fluxes, we used the following expression

$$X_{\text{flux}} = (\Delta C_{\text{sp}} - \Delta C_{\text{med}})/\Delta T \quad (1)$$

where ΔC_{sp} is the change in the concentration of metabolite X in specific species samples while ΔC_{med} is the change in the concentration of metabolite X in medium samples between t = 0 and 72 h, such that ΔT = 72 h. This expression ensures that the effect of medium evaporation and instrumental batch effect are normalized, limiting artifacts of the potential boundary flux profile. To determine the significance of the concentration differences, we employed paired sample tests (Student t-test) with α = 0.05. For each metabolite that exhibited significantly different concentrations between 0 and 72 h, boundary flux values were calculated using eq 1. The standard deviation (STD) was calculated by taking the square root of the sum of the standard variance of concentration at 0 and 72 h, divided by time. This gives the error in the flux value estimated using eq 1. Taking the mean of multiple flux values calculated for the same metabolite gives the average flux value, and total STD is the square root of sum of variance for each flux value. The z-score was calculated by computing the difference in metabolite intensity between the sample and control at each time point (0 and 72 h) and dividing it by the STD of the difference data. The treatments containing only U-^{12}C Glucose or U-^{12}C Glycerol yielded no previously undescribed metabolic phenotypes. We therefore focused our analysis on growth media containing both carbon sources: U-^{12}C Glucose and U-^{12}C Glycerol, U-^{12}C Glucose and U-^{13}C Glycerol, or U-^{13}C Glucose and U-^{12}C Glycerol. These media represent essentially the same nutrient conditions but with different isotopic

https://doi.org/10.1021/acs.analchem.3c04501
Anal. Chem. 2024, 96, 3382−3388

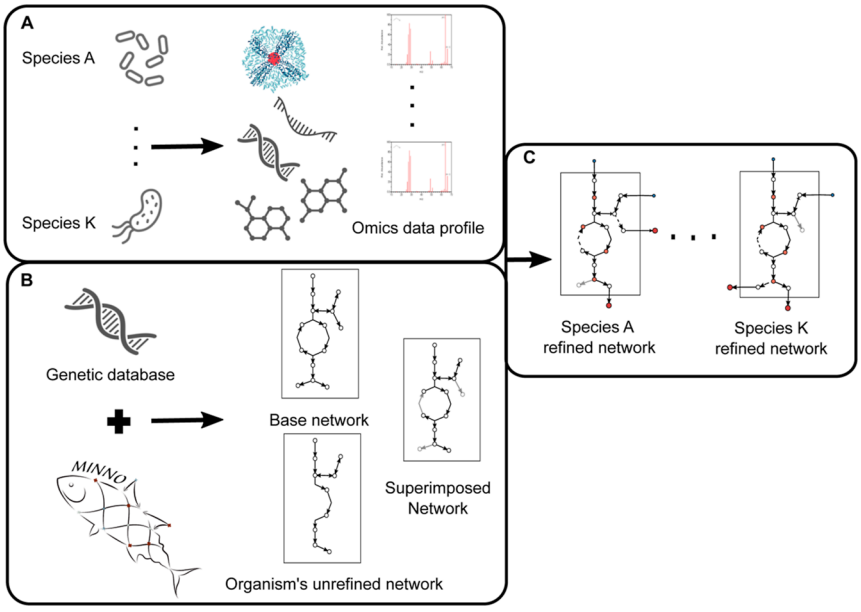

Figure 1. Schematic representation of the metabolic network refinement method. (A) Omics data profiles are produced for species of interest. (B) Using a genetic database (NCBI refSeq) and MINNO, organism-specific metabolic networks are constructed. (C) Refined metabolic networks are created using (B) organism-specific metabolic networks and (A) experimentally generated omics data.

compositions, enabling the determination of the isotope distribution within the cell during growth.

RESULTS AND DISCUSSION

Strategy: Network and Data Visualization Using MINNO. The MINNO visualization tool facilitates both the investigation and understanding of the complex interplay between genotypic and phenotypic features in omics data. MINNO is a JavaScript-based web application that is compatible with Google Chrome and Mozilla Firefox browsers. It uses the D3.js JavaScript library to create dynamic interactive visualizations in web browsers.[30] The tool can load files, such as network files and data files, in JSON, XML, and CSV file formats, while it exports data in JSON, XML, PNG, and SVG formats for multiple applications. It has numerous built-in features that facilitate the creation of detailed network visualizations without the need to switch from multiple editing software tools. More details about MINNO can be found in the user manual that includes a tutorial developed for users to familiarize themselves with many of the tool's features. MINNO is available open-source (under the MIT open-access license) at www.lewisresearchgroup.org/software.

MINNO comes with 66 base metabolic pathways from the KEGG database,[31] covering all primary metabolic pathways that can be combined to build large-scale metabolic networks that include user-added reactions and features. Users can then superimpose an organism's known metabolic pathway data from the KEGG database on these base metabolic pathways without the need to rebuild a network from scratch for each organism studied. The tool can also access metabolic network models from the Biochemical, Genetic, and Genomic (BiGG) database and the NCBI-Reference Sequence (RefSeq) database (available at https://www.ncbi.nlm.nih.gov/refseq/).[32] The tool accepts multiomics data, such as metabolomics, proteomics, and fluxomics data, which can be integrated and visualized on the nodes and edges of the metabolic network. MINNO utilizes empirical data to facilitate the identification of missing reactions by providing users with the ability to investigate reactions pathway-by-pathway or by individual modules. The concept of modularity plays a crucial role in this process. Metabolic networks exhibit modularity as a network property, wherein a module or pathway consists of densely interconnected nodes compared to connections between different modules.[33,34] This modular structure enables the detection of missing reactions within metabolic networks by ensuring that nodes within each module are interconnected with either each other or the surrounding environment. The concept of modularity is a fundamental aspect of metabolic networks and can be applied to metabolic networks of any species. However, except for a handful of model organisms, there are thousands of understudied species that have poorly constructed metabolic networks due to homology mismatch issues. The KEGG database currently includes over 8794 species along with their respective metabolic pathways.[31] By providing access to this extensive information, MINNO allows users to refine metabolic networks and explore individual species or interactions among multiple species.

Network Refinement Strategy. In this example, we used MINNO for our metabolic network refinement strategy to understand metabolic differences among related microbial pathogens (Figure 1). In the context of microbial growth, our strategy involves first culturing microbes *in vitro* and then sampling the cultures over specific time intervals so that metabolite intensities can be recorded as a function of time (Figure 1A). The MINNO visualization tool takes metabolic base/ortholog network layout data from the KEGG database and genetic annotation data from NCBI Reference Sequence database (NCBI-RefSeq) to generate the organism's specific metabolic pathway (Figure 1B). This approach facilitates the identification of potential missing reactions in the organism's metabolic network, shown as gray edges. The user can then incorporate temporal metabolite intensity profiles and intra- or extracellular data onto the network to infer missing reactions by considering boundary fluxes and, if available, the isotope labeling pattern, without resorting to complex mathematical

https://doi.org/10.1021/acs.analchem.3c04501
Anal. Chem. 2024, 96, 3382−3388

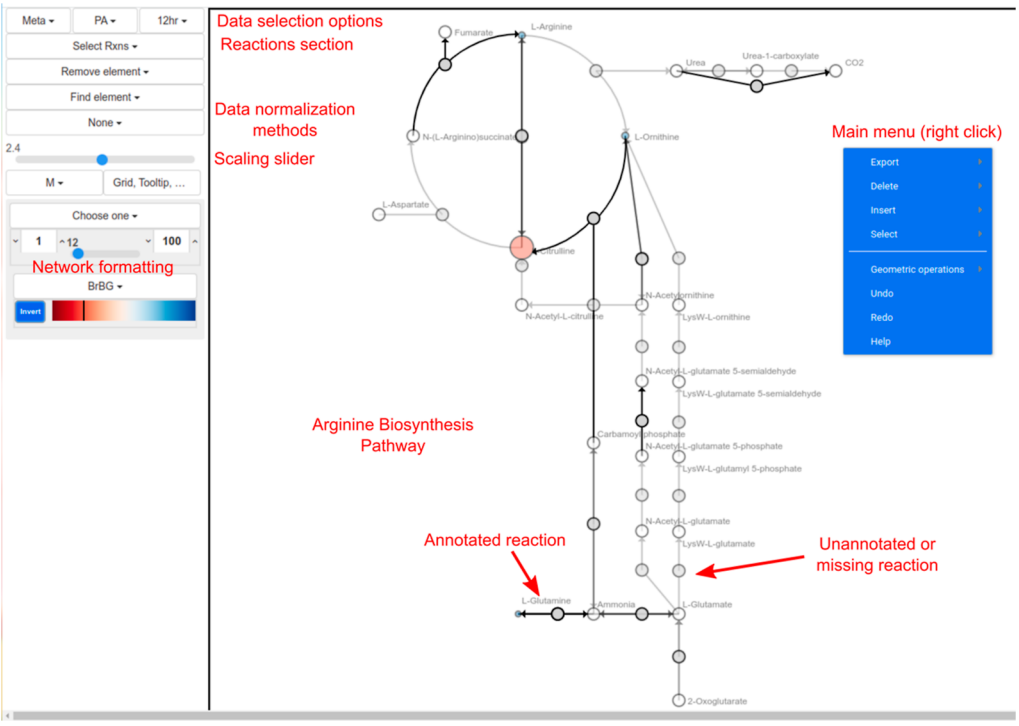

Figure 2. MINNO web-browser interface with key features highlighted in red.

modeling (Figure 1C). In this figure, the dashed links represent the missing reactions inferred by the user.

Users can then search for genes and proteins corresponding to missing reactions using experimental or bioinformatics methods. This approach allows users to refine the networks of under-studied species such as *Borrelia spp.* and find the necessary reactions to explain the metabolic profiles that were missing from their original annotated networks. MINNO can also be used for multiomics data integration as it can incorporate gene, protein, metabolite, and flux data on the same metabolic network.

MINNO User Interface. Figure 2 highlights some key features of the web-based application MINNO. The built-in menu is located on the left side of the screen, where users can select base metabolic pathways from the KEGG database. Later, users can customize the network by dragging and aligning nodes in the network. Additionally, the tool shows organism-specific metabolic networks using genetic annotation information from NCBI-RefSeq database, which show annotated reactions as dark nodes and edges, while unannotated/missing reactions are depicted by light gray nodes and edges. This enables the user to determine the potential missing reactions after experimental data are uploaded onto the network.

Refining Nucleotide Metabolic Pathways Using MINNO. We used MINNO to perform a metabolic network refinement analysis of three *Borrelia* species known to cause Lyme and relapsing fever diseases. By leveraging the modularity concept of metabolic networks and employing boundary flux analysis, we were able to identify the missing reactions from the KEGG database for these species.

The purine metabolism of *B. burgdorferi* in the KEGG database is fragmented, as depicted by solid links in Figure S1A, as it lacks the classic purine salvage pathway.[35] The consumption of both adenine and guanine by *B. burgdorferi* suggests the presence of purine transporters, which has recently been reported in the literature.[36−38] By analyzing the boundary fluxes of cultured cells, we have identified missing reactions in purine metabolism from the KEGG database, indicated by dashed links in Figure S1A. The thickness of the edges represents boundary flux values, while the internal curved arrows pointing toward the biomass indicate the flux directed to DNA and RNA synthesis. This accounts for 35% for adenine and thymine and 15% for guanine and cytosine, based on the A, T, G, and C composition in DNA of *B. burgdorferi*. In contrast, the pyrimidine pathway for *B. burgdorferi* is relatively less fragmented in the KEGG database, as shown by solid links in Figure S1A. However, the boundary flux profile of this species suggests the presence of pyrimidine-nucleoside phosphorylase (*PnP*) based on the production of thymine from thymidine, as shown in Figure S1A, which is missing in the KEGG database. Additionally, *B. burgdorferi* lacks ribonucleotide reductase, an enzyme responsible for converting ribonucleotides (for RNA synthesis) into deoxyribonucleotides (for DNA synthesis).[35] According to our data, *PnP* salvages deoxyribose sugars from thymidine for DNA synthesis. In summary, we used MINNO and empirical metabolomics data to identify eight reactions that are missing from the KEGG database. Subsequent publications have confirmed six of these missing purine reactions (Table S1). Furthermore, MINNO predicted four missing pyrimidine metabolism reactions from the KEGG database, all of which are supported by the primary literature (Table S1).

Metabolic Distinction between *Borrelia* Species Causing Lyme Disease and Relapsing Fever. To better understand metabolic differences between *Borrelia* species, we focused on refining the metabolic networks of *Borrelia* species associated with relapsing fever: *B. parkeri* and *B. turicatae*. These species share genetic similarities, and as expected, their boundary flux profiles exhibit similarities as well[24] (Figures 3 and S1B,C).

https://doi.org/10.1021/acs.analchem.3c04501
Anal. Chem. 2024, 96, 3382−3388

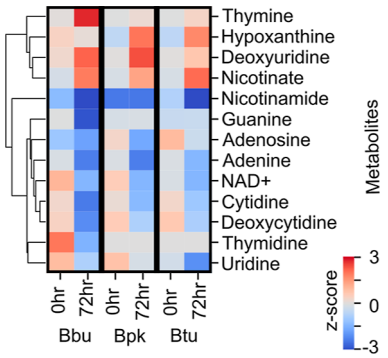

Figure 3. Heatmap showing the temporal profile of selected metabolite intensities across three *Borrelia* species, bbu: *B. burgdorferi*, bpk: *B. parkeri* and btu: *B. turicatae*with respect to the growth medium at 0 and 72 h. The change in metabolite intensity across two different time points (0 and 72 h) has a *p*-value <0.01, and the row *z*-score is shown through the color legend.

Similar to the purine metabolism of *B. burgdorferi*, purine metabolism of both *B. parkeri* and *B. turicatae* is fragmented, as shown as solid links in Figure S1B,C. However, unlike *B. burgdorferi*, both possess the classic purine salvage pathway. They both consume adenosine and adenine, and any excess purine is excreted as hypoxanthine. Interestingly, neither of the isolates studied has an annotated ribonucleotide reductase in the KEGG database. However, based on their boundary flux profiles, we anticipate that both *B. parkeri* and *B. turicatae* harbor a ribonucleotide reductase (*rnr*) (Figure S1B,C).

Metabolic Similarities between *Borrelia* Species Causing Lyme and Relapsing Fever Diseases. It is worth noting that the three *Borrelia* species studied here also shared metabolic similarities. One common feature observed in all three species is the absence of the *thyX* gene in the KEGG database, as shown in Figure S1. The *thyX* gene is essential in all three species for providing the necessary deoxyribonucleosides required for DNA synthesis. Another notable similarity is their deficiency in various biosynthetic pathways essential for the production of nicotinate and nicotinamide. This deficiency highlights their reliance on salvaging precursors for NAD(P) synthesis from the host or the surrounding environment. Our observations revealed that all three *Borrelia* species consume nicotinamide while excreting nicotinate out of the cells, as shown in Figure 4. Notably, the net excretion of nicotinate exceeds the level of nicotinamide consumed for each isolate. This suggests the possible presence of nicotinamide-nucleotide amidase (*pncC*). This salvage process also leads to the generation of essential molecules like PRPP and ATP, as well as the accumulation of ammonia.

In summary, we used MINNO to predict six reactions in purine metabolism for *B. parkeri* and *B. turicatae* that were missing from the KEGG database, with four of these predictions supported by the primary literature (Table S1). MINNO was also used to identify two missing reactions in the KEGG database from the pyrimidine metabolism, although none of them are currently supported by the primary literature. However, these predictions are supported based on homology matches through the PGAP pipeline from NCBI-RefSeq. For nicotinate metabolism, we predicted one reaction shared by all three *Borrelia* species, which is missing from the KEGG database (Table S1).

Summary of Functionality and Applications. Overall, MINNO enables users to refine metabolic networks and integrate multiomics data to provide a system level view of metabolic homeostasis. MINNO's modular approach, whereby discrete metabolic pathway modules can be easily merged together, facilitates the creation of metabolic networks in diverse nonmodel organisms. It also allows users to visualize data on these merged metabolic pathways quickly and easily, without any coding required, facilitating a deeper understanding of complex multiomics data in the context of the broader metabolic system. MINNO can support a variety of applications, such as FBA visualization to model more sophisticated genome-scale behaviors,[39] mapping metabolic architecture in complex microbiome communities,[40] investigating interspecies "cross-talking" interactions,[41,42] and determining the molecular mechanisms of novel antibiotics.[43]

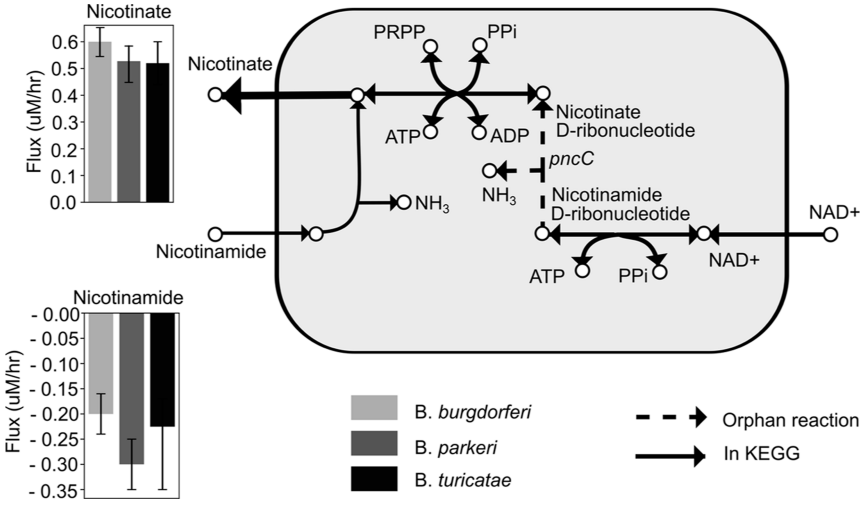

Figure 4. Refined nicotinate and nicotinamide metabolism. Solid links are annotated in the KEGG database, while dashed links represent orphan reactions. Abbr. PRPP: phosphoribosyl pyrophosphate, PPi: diphosphate, and NAD+: nicotinamide adenine dinucleotide. The error bars represent standard deviation (sample size $n = 3$).

https://doi.org/10.1021/acs.analchem.3c04501
Anal. Chem. 2024, 96, 3382−3388

CONCLUSIONS

Here, we introduce MINNO, a new software tool that allows researchers to integrate genomic and empirical metabolomics data into a single software environment in order to build and refine metabolic networks. We illustrate the utility of this tool for identifying missing reactions within multiple metabolic pathways for *Borrelia* species. Using MINNO, we identified 18 missing reactions from the KEGG database, of which nine were supported by the primary literature. The remaining reactions show good homology as in the NCBI-RefSeq database (Table S1). MINNO provides a tool that can be applied to any organism to systematically refine or investigate metabolic pathways. MINNO was designed to be inherently flexible for these diverse applications and support a wide range of input formats. We anticipate that it will be a useful asset for analyzing genome-wide knockouts, studying novel organisms that are divergent from typical model organisms, metabolic flux analysis, and visualization of metabolic networks.

ASSOCIATED CONTENT

Data Availability Statement

Code availability: MINNO is available for free use (under the MIT license) on GitHub- https://lewisresearchgroup.github.io/MINNO/ as Lewis Research Group (LRG) software. Freely available on www.lewisresearchgroup.org/software

Supporting Information

The Supporting Information is available free of charge at https://pubs.acs.org/doi/10.1021/acs.analchem.3c04501.

Refined purine and pyrimidine metabolism of *Borrelia* species and missing reactions identified for *Borrelia* species (PDF)

Raw intensities for metabolites (XLSX)

Standard curve parameters for converting intensities to concentrations (XLSX)

Boundary flux values determined from concentrations (XLSX)

AUTHOR INFORMATION

Corresponding Authors

Ian A. Lewis − *Alberta Centre for Advanced Diagnostics, Department of Biological Sciences, University of Calgary, Calgary T2N 1N4 Alberta, Canada;* orcid.org/0000-0002-5753-499X; Phone: +1 403 220 4366; Email: ian.lewis2@ucalgary.ca

Jörn Davidsen − *Department of Physics and Astronomy, University of Calgary, Calgary T2N 1N4 Alberta, Canada; Hotchkiss Brain Institute, University of Calgary, Calgary T2N 1N4 Alberta, Canada;* Phone: +1 403 210 7964; Email: davidsen@phas.ucalgary.ca

Authors

Ayush Mandwal − *Department of Physics and Astronomy, University of Calgary, Calgary T2N 1N4 Alberta, Canada*

Stephanie L. Bishop − *Alberta Centre for Advanced Diagnostics, Department of Biological Sciences, University of Calgary, Calgary T2N 1N4 Alberta, Canada;* orcid.org/0000-0002-8134-7297

Mildred Castellanos − *Department of Biochemistry and Molecular Biology, Cumming School of Medicine, Snyder Institute for Chronic Diseases, University of Calgary, Calgary T2N 1N4 Alberta, Canada*

Anika Westlund − *Alberta Centre for Advanced Diagnostics, Department of Biological Sciences, University of Calgary, Calgary T2N 1N4 Alberta, Canada*

George Chaconas − *Department of Biochemistry and Molecular Biology, Cumming School of Medicine, Snyder Institute for Chronic Diseases and Department of Microbiology, Immunology and Infectious Diseases, Cumming School of Medicine, Snyder Institute for Chronic Diseases, University of Calgary, Calgary T2N 1N4 Alberta, Canada*

Complete contact information is available at: https://pubs.acs.org/10.1021/acs.analchem.3c04501

Author Contributions

A.M. and S.L.B. contributed equally to this manuscript. Ayush Mandwal—conceptualization, formal analysis, data curation, software, methodology, validation, and writing—original draft. Stephanie L. Bishop—conceptualization, validation, methodology, experimental, and writing—original draft. Mildred Castellanos—experimental. Anika Westlund—validation. George Chaconas—validation, funding acquisition, and writing—review and editing. Ian Lewis—conceptualization, supervision, validation, funding acquisition, and writing—review and editing. Jörn Davidsen—supervision, funding acquisition, and writing—review and editing.

Notes

The authors declare no competing financial interest.

ACKNOWLEDGMENTS

We thank Soren Wacker for providing necessary support in deploying the web application on GitHub for public use. This work was financially supported by the Natural Sciences and Engineering Research council of Canada (NSERC) through a Discovery Grant to J.D. (DG 05221). I.A.L. is supported by an Alberta Innovates Translational Health Chair and a grant from the Natural Sciences and Engineering Research Council of Canada (NSERC; DG04547). S.L.B. is supported by a National Institutes of Health (NIH) grant (project number 1R01AI153521-01) and a Canadian Institutes of Health Research (CIHR) Postdoctoral Fellowship (project number 202110HIV-477488-87373). This work was also supported by the Canadian Institutes for Health Research operating grants PJT-153336 and PJT-180584 to G.C. Metabolomics data were acquired at the Calgary Metabolomics Research Facility, which is part of the Alberta Centre for Advanced Diagnostics (ACAD; PrairiesCan RIE #22734) and is supported by the International Microbiome Centre and the Canada Foundation for Innovation (CFI-JELF 34986).

REFERENCES

(1) Johnson, C. H.; Ivanisevic, J.; Siuzdak, G. *Nat. Rev. Mol. Cell Biol.* **2016**, *17*, 451−459.
(2) Bishop, S. L.; Drikic, M.; Wacker, S.; Chen, Y. Y.; Kozyrskyj, A. L.; Lewis, I. A. *Mucosal Immunol.* **2022**, *15*, 1071−1084.
(3) Wilson, D. F.; Matschinsky, F. M. *Front. Physiol.* **2021**, *12*, 486.
(4) Peregrín-Alvarez, J. M.; Sanford, C.; Parkinson, J. *Genome Biol.* **2009**, *10*, R63.
(5) Peregrin-Alvarez, J. M.; Tsoka, S.; Ouzounis, C. A. *Genome Res.* **2003**, *13*, 422−427.
(6) Wagner, A. Metabolic networks and their evolution. *Evolutionary Systems Biology*; Springer, 2012; Vol. *751*, pp 29−52.
(7) Li, W.; O'Neill, K. R.; Haft, D. H.; DiCuccio, M.; Chetvernin, V.; Badretdin, A.; Coulouris, G.; Chitsaz, F.; Derbyshire, M.; Durkin, A. S.; et al. *Nucleic Acids Res.* **2021**, *49*, D1020−D1028.

(8) Haft, D. H.; DiCuccio, M.; Badretdin, A.; Brover, V.; Chetvernin, V.; O'Neill, K.; Li, W.; Chitsaz, F.; Derbyshire, M. K.; Gonzales, N. R.; et al. *Nucleic Acids Res.* **2018**, *46*, D851−D860.
(9) Lee, D.; Redfern, O.; Orengo, C. *Nat. Rev. Mol. Cell Biol.* **2007**, *8*, 995−1005.
(10) Schnoes, A. M.; Brown, S. D.; Dodevski, I.; Babbitt, P. C. *PLoS Comput. Biol.* **2009**, *5*, No. e1000605.
(11) Jones, C. E.; Brown, A. L.; Baumann, U. *BMC Bioinf.* **2007**, *8*, 170.
(12) Yarmosh, D. A.; Lopera, J. G.; Puthuveetil, N. P.; Combs, P. F.; Reese, A. L.; Tabron, C.; Pierola, A. E.; Duncan, J.; Greenfield, S. R.; Marlow, R.; et al. *mSphere* **2022**, *7*, No. e00077-22.
(13) King, Z. A.; Dräger, A.; Ebrahim, A.; Sonnenschein, N.; Lewis, N. E.; Palsson, B. O. *PLoS Comput. Biol.* **2015**, *11*, No. e1004321.
(14) Chazalviel, M.; Frainay, C.; Poupin, N.; Vinson, F.; Merlet, B.; Gloaguen, Y.; Cottret, L.; Jourdan, F. *Bioinformatics* **2018**, *34*, 312−313.
(15) Droste, P.; Nöh, K.; Wiechert, W. *Chem. Ing. Tech.* **2013**, *85*, 849−862.
(16) Otasek, D.; Morris, J. H.; Bouças, J.; Pico, A. R.; Demchak, B. *Genome Biol.* **2019**, *20*, 185.
(17) Funahashi, A.; Morohashi, M.; Kitano, H.; Tanimura, N. *BIOSILICO* **2003**, *1*, 159−162.
(18) Kutmon, M.; van Iersel, M. P.; Bohler, A.; Kelder, T.; Nunes, N.; Pico, A. R.; Evelo, C. T. *PLoS Comput. Biol.* **2015**, *11*, No. e1004085.
(19) Stanek, G.; Strle, F. *FEMS Microbiol. Rev.* **2018**, *42*, 233−258.
(20) Coburn, J.; Garcia, B.; Hu, L. T.; Jewett, M. W.; Kraiczy, P.; Norris, S. J.; Skare, J. *Curr. Issues Mol. Biol.* **2022**, *42*, 473−518.
(21) Shapiro, E. D. *Pediatr. Rev.* **2014**, *35*, 500−509.
(22) Dworkin, M. S.; Schwan, T. G.; Anderson, D. E. *Med. Clin. North Am.* **2002**, *86*, 417−433.
(23) Purser, J. E.; Norris, S. J. *Proc. Natl. Acad. Sci. U.S.A.* **2000**, *97*, 13865−13870.
(24) Schwan, T. G.; Raffel, S. J.; Schrumpf, M. E.; Policastro, P. F.; Rawlings, J. A.; Lane, R. S.; Breitschwerdt, E. B.; Porcella, S. F. *J. Clin. Microbiol.* **2005**, *43*, 3851−3859.
(25) Barbour, A. G. *Yale J. Biol. Med.* **1984**, *57*, 521.
(26) Rydzak, T.; Groves, R. A.; Zhang, R.; Aburashed, R.; Pushpker, R.; Mapar, M.; Lewis, I. A. *Nat. Commun.* **2022**, *13*, 2332.
(27) Groves, R. A.; Mapar, M.; Aburashed, R.; Ponce, L. F.; Bishop, S. L.; Rydzak, T.; Drikic, M.; Bihan, D. G.; Benediktsson, H.; Clement, F.; Gregson, D. B.; Lewis, I. A. *Anal. Chem.* **2022**, *94*, 8874−8882.
(28) Ausubel, F. M.; Brent, R.; Kingston, R. E.; Moore, D. D.; Seidman, J.; Smith, J. A.; Struhl, K. *Short Protocols in Molecular Biology*; Wiley: New York, 1992; Vol. *275*, pp 28764−28773.
(29) Melamud, E.; Vastag, L.; Rabinowitz, J. D. *Anal. Chem.* **2010**, *82*, 9818−9826.
(30) Bostock, M.; Ogievetsky, V.; Heer, J. *IEEE Trans. Visual. Comput. Graph.* **2011**, *17*, 2301.
(31) Kanehisa, M.; Sato, Y.; Furumichi, M.; Morishima, K.; Tanabe, M. *Nucleic Acids Res.* **2019**, *47*, D590−D595.
(32) King, Z. A.; Lu, J.; Dräger, A.; Miller, P.; Federowicz, S.; Lerman, J. A.; Ebrahim, A.; Palsson, B. O.; Lewis, N. E. *Nucleic Acids Res.* **2016**, *44*, D515−D522.
(33) Ravasz, E.; Somera, A. L.; Mongru, D. A.; Oltvai, Z. N.; Barabási, A. L. *Science* **2002**, *297*, 1551−1555.
(34) Newman, M. E. *Proc. Natl. Acad. Sci. U.S.A.* **2006**, *103*, 8577−8582.
(35) Fraser, C. M.; Casjens, S.; Huang, W. M.; Sutton, G. G.; Clayton, R.; Lathigra, R.; White, O.; Ketchum, K. A.; Dodson, R.; Hickey, E. K.; et al. *Nature* **1997**, *390*, 580−586.
(36) Cuellar, J.; Åstrand, M.; Elovaara, H.; Pietikäinen, A.; Sirén, S.; Liljeblad, A.; Guédez, G.; Salminen, T. A.; Hytönen, J. *Infect. Immun.* **2020**, *88*, No. e00962-19.
(37) Jain, S.; Sutchu, S.; Rosa, P. A.; Byram, R.; Jewett, M. W. *Infect. Immun.* **2012**, *80*, 3086−3093.
(38) Jain, S.; Showman, A. C.; Jewett, M. W. *Infect. Immun.* **2015**, *83*, 2224−2233.
(39) O'Brien, E. J.; Monk, J. M.; Palsson, B. O. *Cell* **2015**, *161*, 971−987.
(40) Gilbert, J. A.; Blaser, M. J.; Caporaso, J. G.; Jansson, J. K.; Lynch, S. V.; Knight, R. *Nat. Med.* **2018**, *24*, 392−400.
(41) Faust, K.; Raes, J. *Nat. Rev. Microbiol.* **2012**, *10*, 538−550.
(42) Mohammadi, M.; Bishop, S. L.; Aburashed, R.; Luqman, S.; Groves, R. A.; Bihan, D. G.; Rydzak, T.; Lewis, I. A. *Front. Microbiol.* **2022**, *13*, 958785.
(43) Kohanski, M. A.; Dwyer, D. J.; Collins, J. J. *Nat. Rev. Microbiol.* **2010**, *8*, 423−435.

https://doi.org/10.1021/acs.analchem.3c04501
Anal. Chem. 2024, 96, 3382−3388